JOURNAL OF VIROLOGY, Apr. 2001, p. 3301–3313 Vol. 75, No. 7
0022-538X/01/$04.00+0 DOI: 10.1128/JVI.75.7.3301–3313.2001

Human Immunodeficiency Virus Type 1 Central DNA Flap: Dynamic Terminal Product of Plus-Strand Displacement DNA Synthesis Catalyzed by Reverse Transcriptase Assisted by Nucleocapsid Protein

LAURENCE HAMEAU,[1] JOSETTE JEUSSET,[1] SOPHIE LAFOSSE,[1] DOMINIQUE COULAUD,[1] ETIENNE DELAIN,[1] TORSTEN UNGE,[2] TOBIAS RESTLE,[3] ERIC LE CAM,[1] AND GILLES MIRAMBEAU[1]*

Laboratoire de Microscopie Moléculaire et Cellulaire, CNRS UMR 8532, Institut Gustave Roussy, 94805 Villejuif Cedex, France[1]; Department of Molecular Biology, University of Uppsala, S-111 11 Uppsala, Sweden[2]; and Abteilung Physikalische Biochemie, Max-Planck-Institut für Molekulare Physiologie, 44227 Dortmund, Germany[3]

Received 5 October 2000/Accepted 20 December 2000

To terminate the reverse transcription of the human immunodeficiency virus type 1 (HIV-1) genome, a final step occurs within the center of the proviral DNA generating a 99-nucleotide DNA flap (6). This step, catalyzed by reverse transcriptase (RT), is defined as a discrete strand displacement (SD) synthesis between the first nucleotide after the central priming (cPPT) site and the final position of the central termination sequence (CTS) site. Using recombinant HIV-1 RT and a circular single-stranded DNA template harboring the cPPT-CTS sequence, we have developed an SD synthesis-directed in vitro termination assay. Elongation, strand displacement, and complete central flap behavior were analyzed using electrophoresis and electron microscopy approaches. Optimal conditions to obtain complete central flap, which ended at the CTS site, have been defined in using nucleocapsid protein (NCp), the main accessory protein of the reverse transcription complex. A full-length HIV-1 central DNA flap was then carried out in vitro. Its synthesis appears faster in the presence of the HIV-1 NCp or the T4-encoded SSB protein (gp32). Finally, a high frequency of strand transfer was shown during the SD synthesis along the cPPT-CTS site with RT alone. This reveals a local and efficient 3′-5′ branch migration which emphasizes some important structural fluctuations within the flap. These fluctuations may be stabilized by the NCp chaperone activity. The biological implications of the RT-directed NCp-assisted flap synthesis are discussed within the context of reverse transcription complexes, assembly of the preintegration complexes, and nuclear import of the HIV-1 proviral DNA to the nucleus toward their chromatin targets.

During the few last years, it has been shown that the plus-strand DNA synthesis step of lentiviruses differs significantly from that of other retroviruses. This step terminates by a strand displacement (SD) synthesis of~99 nucleotides (nt) at the center of the genome, which generates a central DNA flap corresponding to a three-stranded structure with two overlapping positive-strand segments (6, 44). This central flap synthesis appears to be important for the replication of human immunodeficiency virus type 1 (HIV-1) in nondividing cells, since mutants altering its formation are defective in their replication (5, 6, 22). Nuclear import of the proviral DNA is impaired with these mutants, while some HIV-derived vectors supporting the central flap synthesis are activated for genetic transduction (12, 53). With such an impact, the HIV-1 central DNA flap requires now a complete characterization (45).

The different steps leading to the central flap formation during the lentiviral plus-strand DNA synthesis are summarized in Fig. 1. This model is based on ex vivo experiments that showed full-length nonintegrated linear DNA molecules extracted from HIV-1-infected cells containing a central discontinuity on the plus strand (4, 6, 21, 44). The plus-strand DNA synthesis is initiated from a couple of canonical polypurine tracts (PPTs), which are resistant against the nucleolytic degradation activity of the reverse transcriptase (RT)-associated RNase H (37, 38, 39). The universal one flanking the 3′ element U3R is referred to as the 3′PPT primer, and the other one, located at the center of the RNA chain, is referred to as the cPPT primer. These two RNA sequences are efficient primers for a discontinuous double initiation of the plus-strand synthesis (4, 5, 21, 22, 27). The upstream strand initiated at the 3′PPT is elongated through the cPPT, and by a mechanism of strand displacement, up to a nearby site located 80 to 100 nt downstream, referred as the central termination sequence (CTS). CTS is extremely efficient in terminating HIV-1 RT-catalyzed DNA elongation, whereas RT only pauses at this stop signal in absence of SD synthesis (6, 28). This drastic effect results from severe distortions within the nascent double helix located in the CTS closely upstream of the discrete pausing sites (ter0, ter1, and ter2 loci), which gradually force RT to pause and then to dissociate as it reaches these sites. A series of AnTm stretches found within the CTS box are the key elements, as their base pairs are stacked in a way that generates a compressed minor groove in a highly rigid and bent helix, which clearly affects the binding of RT to DNA (28, 29). Coupling this CTS property with the double-initiation strategy leads to a termination of plus-strand DNA synthesis with a

* Corresponding author. Mailing address: Laboratoire de Microscopie Moléculaire et Cellulaire, CNRS UMR 8532, Institut Gustave Roussy, 94805 Villejuif Cedex, France. Phone: 331-42-11-48-80. Fax: 331-42-11-52-76. E-mail: mirambe@igr.fr.

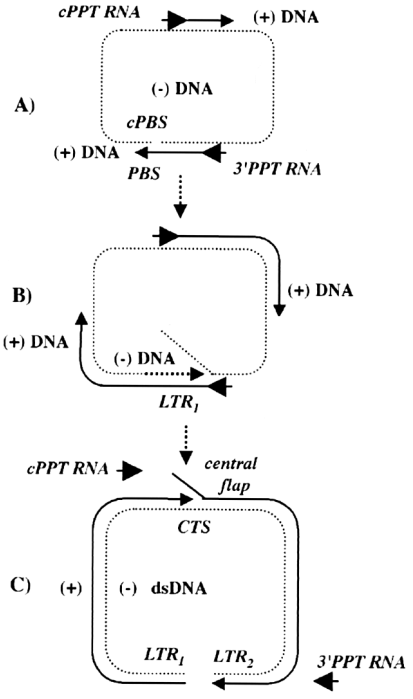

FIG. 1. Simplified model of HIV-1 plus-strand DNA synthesis. The two PPT RNA primers are the two constitutive primers of plus-strand DNA synthesis. RT is not shown for clarity. (A) The 3′PPT-primed plus-strand DNA is transferred from one end of the minus-strand DNA template to the other end (complementary to the PBS sequence), while a cPPT-primed plus-strand DNA is normally extended. (B) The two PPT-primed plus-strand DNAs are further elongated, while minus-strand DNA is completed with an SD synthesis which forms the first dsLTR (LTR_1). (C) The full-length DNA is produced with the two LTRs (LTR_1 and LTR_2), the central flap (with a SD synthesis initiated at the cPPT and blocked at the CTS site), and without the two PPT RNAs, separated from the DNA by RNase H and SD synthesis. The real chronology between the final steps and its possible consequences are still unclear. As SD synthesis is at least 10 times slower than simple synthesis in vitro with RT alone, SD synthesis may occur at the same time to generate the LTR_1 and the central flap. SD synthesis may also occur in the LTRs with two SD-converging RTs, one elongating the minus-strand DNA (LTR_1) and the other one elongating the plus-strand DNA (LTR_2) at the same time (49). However, repetitive pausing during the course of the normal two PPT-primed plus-strand DNA synthesis and the strong pausing in the CTS to reach the ultimate position (ter2) would favor the central flap to be processed at the end of the reaction. Otherwise, secondary priming sites may occur with a low frequency to perform the plus-strand DNA, generating then some nonconstitutive sites of SD synthesis (27).

~99-nt DNA flap located at the center of the proviral DNA (6).

The final steps of HIV-1 reverse transcription clearly consist of both long terminal repeat (LTR) duplication and central flap synthesis, two steps requiring SD synthesis (Fig. 1). They must occur within the nucleoproteic reverse transcription complex (RTC), including at least RT and the nucleocapsid protein (NCp) as the active protein components (46). Synthesis of the flap has not yet been studied in the RTC context. The HIV-1 NCp effect is not so clear for the 650-nt SD synthesis within the LTR sequence: one study showed a positive effect, whereas a second one did not (1, 14). All of the preceding steps of reverse transcription were shown in vitro to be enhanced by NCp. NCp promotes the primer-binding site (PBS)-directed initiation of minus-strand DNA (34), the transfer of minus-strand strong stop DNA in vitro (19, 38), the processivity of DNA synthesis (23), the RNase H activity of RT (3, 38), and the transfer of the plus-strand strong stop DNA (51). To assist most of these reactions, NCp acts as a nucleic acid chaperone, combining helix-destabilizing and strand-annealing properties (41, 47). In addition, protein-protein interactions between NCp and RT are critical (9, 33). Some effects of one or more additional auxiliary protein(s) have also been proposed to be involved within the RTC complexes. For instance, the HIV-1 proteins Vpr and integrase are enhancing the fidelity of DNA synthesis and the efficiency of the tRNAlys3-directed initiation, respectively (35, 52). Concerning the in vitro SD synthesis, the human SSB protein RP-A has been shown to stimulate it along the LTR sequence (1, 15), when the HIV-1 RT is less active than the Moloney murine leukemia virus (MMLV) RT to carry out this reaction alone (50). On the other hand, the transition from RTCs to preintegration complexes (PICs) implies a change in the distribution of the proteins associated with the retroviral genome (11, 24), progressively converted from two RNA molecules to one linear double-stranded DNA (dsDNA). The SD synthesis, which delineates both the final steps of reverse transcription and the DNA sites (central DNA flap and LTRs) that are necessary for the PIC activities, is then an important process to be analyzed. It may dynamically direct the association of some protein-DNA complexes engaged in the PIC assembly or in the necessary interaction between PICs and the associated cellular processes. To date with respect to the HIV-1 central flap being a product of SD synthesis, few data are available about its biochemical properties. Generating this flap in vitro is associated with a recombinatory process, relevant to the strand displacement reaction (16), while an artificial flap harboring a part of the central HIV-1 sequence is repaired in vitro by the human flap nuclease FEN-1 (42).

Taking into account these data and hypotheses, we present here the first in vitro assay that mimics the HIV-1 central termination of plus-strand DNA synthesis in order to generate a complete central flap. We have optimized and analyzed the synthesis of DNA flaps catalyzed by HIV-1 RT on a circular single-stranded DNA (ssDNA) template containing the HIV-1 central minus-strand DNA sequence (Fig. 2). Furthermore, we have investigated the effects on flap synthesis of two efficient ssDNA-binding proteins: the HIV-1 partner, i.e., NCp, and the paradigmatic helix-destabilizing protein, i.e., the T4-encoded single-stranded binding protein (SSB) gp32.

MATERIALS AND METHODS

Materials. Recombinant HIV-1 RT (heterodimer, p66-p51) was expressed in *Escherichia coli* and purified as described before (36, 48). Enzyme concentrations were routinely determined using an extinction coefficient at 280 nm of 260, 450 M^{-1} cm^{-1}. The purified enzymes were stored at −70°C in aliquots with a fixed concentration of 1 mg/ml. The concentration of active enzyme was estimated as 5 μM. NC protein (1–55) was obtained from L. H. Henderson (National Cancer Institute, Frederick, Md.). Sequenase version 2.0 DNA sequencing kit was obtained from U.S. Biochemical Corp., [γ-^{33}P]ATP (3,000 Ci/mmol) was from ICN, and T4 polynucleotide kinase and gp32 were from AP Biotech. *Bsp*MI and *Sma*I enzymes were provided by New England Biolabs. The chemicals used in this study correspond to the best grade and were purchased from established manufacturers.

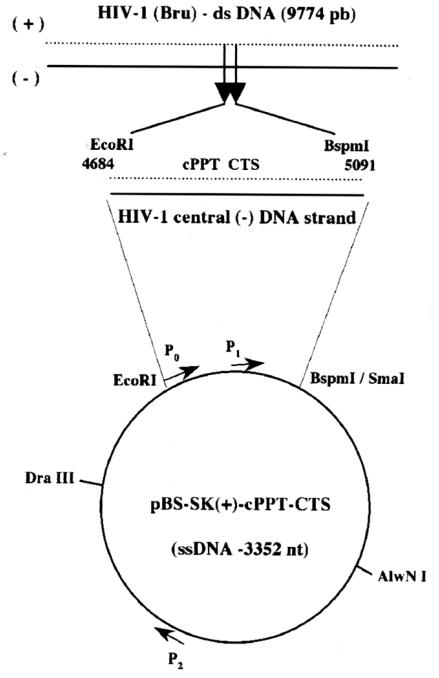

FIG. 2. Strategy to mimic the plus-strand DNA synthesis. The *Eco*RI/*Bam*HI fragment of the HIV-1 Bru DNA, containing the cPPT and CTS sequences, is inserted in a pBluescript SK(+) phagemid DNA. This generates the single-stranded model substrate pBS-SK(+)–cPPT-CTS used as a template for HIV-1 RT. For the experiments described in this study, the primers P_0, P_1, and P_2 were used. These primers are 17-mer oligodeoxyribonucleotides corresponding to the 5′ region of the *Eco*RI site (P_0), the 5′ end of the central flap (P_1), and the 5′ region of the *Sca*I site (P_2), respectively. P_0 and P_2 are located 134 and 1,293 nt upstream of P_1, respectively.

Constructions. The *Eco*RI-*Eco*RI fragment of double-stranded pBru HIV-1 DNA (Pasteur Institute, Paris, France) was inserted into the pBluescript SK(+) phagemid (Stratagene). The recombinant DNA was then digested with *Bsp*MI (within the HIV-1 sequence) and *Sma*I [within the SK(+) polylinker]. The 3′-*Bsp*MI overhangs were filled up with *Taq* DNA polymerase to generate blunt ends. Intramolecular ligation with the *Sma*I blunt ends yielded a circular DNA of 3,352 bp, containing 402 bp derived from the HIV-Bru sequence (Fig. 2). Circular plasmid DNA (SK-PPT-CTS) was purified by cesium chloride density gradient centrifugation in the presence of ethidium bromide (43). Circular phage DNA was prepared using the M13 ssDNA purification protocol (43) after phage production using the helper phage R408 (Stratagene). The ssDNA was further purified by gel filtration on a Superose 6B Micro-Column in 400 mM NaOH using a SMART system (AP Biotech) and then on μ-Spin 400 columns (AP Biotech) to ensure separation from phage coat proteins and contaminating primers. The purified DNA was then analyzed by agarose gel and electron microscopy.

Primers and hybrids. The oligonucleotides used in the experiments were purchased from Eurogentec or Genset. The sequences are as follows: P_0 (DNA, 18 mer, 5′-AATTCCCTACAATCCCCA), P_1 (DNA, 17 mer, 5′-TTGGGGGG TACAGTGCA), P_2 (DNA, 17 mer, 5′-GAGTACTCAACCAAGTC), and cPPT (RNA, 16 mer, 5′-AAAAGAAAAGGGGGGA). The oligonucleotides were purified on 20% polyacrylamide–7 M urea gels in TBE buffer (10 mM Tris-borate [pH 8.0] and 1mM EDTA). The P_0 primer was 5′ end labeled with ^{33}P using [γ-^{33}P]ATP and T4 polynucleotide kinase (AP Biotech) according to the manufacturer's instructions and purified with μ-Spin G25 columns (AP Biotech). The hybrids were prepared by mixing the template and one unlabeled primer (P_1 or P_2) at a 1:5 molar ratio or the template with the labeled P_0 primer with or without the unlabeled primer (P_1 or cPPT) at a 1:1 or 1:1:5 molar ratio in 50 mM Tris-acetate (pH 7.8), 50 mM sodium acetate, and 6 mM magnesium diacetate for 3 min at 90°C, followed by 30 min at 60°C, and then cooled down to room temperature. Complete hybridization was confirmed on native polyacrylamide gels.

Extension from the ^{33}P-labeled P_0 primer to observe SD synthesis along the cPPT-CTS region. The preannealed primer-template substrate (5 to 10 nM) was incubated at 37°C with HIV-1 RT (4 to 150 nM) in a buffer containing 50 mM Tris-acetate (pH 7.8), 50 mM Sodium acetate, 6 mM Magnesium diacetate, and 25 to 100 μM deoxynucleoside triphosphates (dNTPs). Incubation times and deviations from the above standard reaction conditions are indicated within the figure legends. The reactions were always stopped by adding EDTA at a final concentration of 50 mM. The samples were then diluted with formamide loading buffer including xylene cyanol and bromphenol blue (95% formamide after sample evaporation). Alternatively, the DNA products were extracted with phenol-chloroform-isoamyl alcohol and 1% sodium dodecyl sulfate, precipitated in ethanol, and centrifuged and the pellets were dissolved in the loading buffer. The samples were heated for 5 min at 90°C before loading them onto an 8% acrylamide gel containing 7 M urea. Electrophoresis was performed at 70 W until the bromphenol blue dye reached the bottom. Finally, the gel was dried at 80°C, exposed for 4 to 24 h, and scanned using phosphorimager technology (PhosphorImager and ImageQuant; Molecular Dynamics).

Complete DNA synthesis followed by SD synthesis along the 3,352-nt circular ssDNA. Primers P_1 or P_2 were annealed to the ssDNA, and the polymerase reaction was carried out as described above. Typically, the products were analyzed in 1% agarose gel electrophoresis, followed by fluorescence detection. To optimize nucleic acid migration, 1% lithium dodecyl sulfate (LDS) was added. Single- and double-stranded DNA species were stained with SYBR Green I, as recommended by the manufacturer (Molecular Probes), and detected at 254 nm using an UV transilluminator. Photographs of the images were taken with a standard Polaroid apparatus. In order to follow the pausing profile after one round of synthesis, the products were digested with *Eco*RI to generate a 5′ end on the nascent strand (corresponding to a P_0-like primed DNA). The 5′ ends were then labeled using a standard procedure. First, the 5′ phosphates were removed with calf intestine phosphatase (CIAP), followed by [γ-^{33}P]ATP labeling with T4 polynucleotide kinase. The DNA products were then loaded onto an 8% acrylamide gel containing 7 M urea. Electrophoresis was performed as described in the former section. The ssDNA fragments that enter into the gel were exclusively produced by an arrest of SD synthesis.

EM of the circular DNA products. DNA products were purified by gel filtration on a Superose 6B Micro-Column with a SMART system (both AP Biotech) in 10 mM Tris (pH 7.5), 50 mM NaCl, and 1 mM EDTA. To obtain a good spreading of ssDNA, T4 SSB gp32 was added to the DNA solution at a ratio of one gp32 tetramer per 5 nt. Electron microscopy (EM) was performed as described previously (30, 31). First, 5 μl of a DNA solution, at a final concentration of 1μg/ml, was spotted onto a 600-mesh copper grid coated with a very thin carbon film activated by a glow discharge in the presence of pentylamine according to the method of Dubochet et al. (10). Grids were washed with a 2% aqueous uranyl acetate solution, dried, and viewed in the annular dark-field mode, using a LEO-Zeiss 902 electron microscope. Individual molecules were directly analyzed at a final magnification of ×340,000 on a Kontron Image Analysis System connected to the microscope through a video camera. Contour length measurements of the DNA were done by using the *x* and *y* coordinates obtained by digitization of the DNA images.

RESULTS

Overall strategy: primer elongation along a circular ssDNA template. In order to analyze the central termination process, an HIV-1 DNA fragment containing the cPPT-CTS sequence was inserted into a Bluescript phagemid DNA (Fig. 2). Purification of the recombinant circular ssDNA from phage suspensions was optimized in order to reduce the level of contaminating coat proteins as well as copurifying primers (see Materials and Methods). This allowed us to analyze the products of DNA synthesis not only with radiolabeled primers but also by fluorescence detection in agarose gels and directly by EM. To study the strand displacement synthesis on the HIV-1 DNA template, we applied two classical approaches of primer extension. The first one uses two adjacent primers: the upstream primer was end labeled, and the elongated strand from the downstream primer generated the strand to be displaced.

The second approach takes advantage of the fact that the template is circular. The primer is first elongated generating a partially double-stranded substrate, and this new strand is then displaced upon further elongation of the DNA template. The reaction resembles a rolling-circle mechanism, which will depend on the efficiency of HIV-1 RT-catalyzed strand displacement synthesis. The tail length of the displaced strand can be analyzed within the flap by band shift assays on agarose gels or more directly by EM after covering the ssDNA with an SSB protein. The polymerase pausing pattern on extended DNA chains can be analyzed by end labeling after an endonuclease digestion of the dsDNA products.

Pausing patterns of HIV-1 RT along the cPPT-CTS negative-strand DNA template. The SD synthesis within the cPPT-CTS locus catalyzed by HIV-1 RT was first observed performing kinetic experiments of primer extension. DNA synthesis was initiated from a labeled primer P_0, located 134 nt upstream the cPPT, in the presence or absence of a strand to be displaced. SD synthesis is initiated by displacing the strand initiated at the primer P_1, located at the 3′ end of the cPPT and corresponding to the 5′ end of the central flap. Different conditions were tested by our assay in order to reduce the distributivity of the reaction. Acetate was substituted for chloride since it gave a slightly better processivity (data not shown). Generally, RT was in two- to sixfold excess over the annealed primers, and dNTPs were added in a large excess (100 μM compared to 5 to 9 nM of template). Figure 3 presents a typical experiment comparing normal and SD synthesis with a twofold excess of RT over substrate.

The strong pausing at ter0, ter1, and ter2 within the CTS site, characterized previously (6, 28), was observed in both situations: normal DNA synthesis compared to SD synthesis. These sites represent the strongest pausing sites under our conditions. Without SD synthesis, the enzyme is able to slowly overcome these pausing sites with increasing time of incubation, with ter2 showing the stronger pause. Upstream of the CTS, two other pausing sites could be revealed. The first one, not shown before, was identified upstream of the cPPT, corresponding to the position 4749 (HIV-1 Bru). The second sequence was located within the cPPT site in an A-repeat, like that already shown (26). During SD synthesis, RT makes additional strong pauses between the cPPT and the CTS. A first pause is normally located at the start of the SD synthesis corresponding to the 5′ end of the downstream strand. A second pause, weaker than the first one, is located within a sequence, where four guanines are to be incorporated. Furthermore, we observed a general slowdown of elongation during SD synthesis. The pauses observed within 3 min of incubation without SD were similar to the pauses observed within 30 min of the SD synthesis. No significant elongation from this pausing sites could be observed even when the reaction was extended to 60 min. Elongation is therefore slowed down ca. 10-fold in the context of SD synthesis compared to normal synthesis. With a high excess of RT and long incubation times, ter2 can be bypassed (data not shown). These results, which for the first time take into account the complete 3′ cPPT-CTS DNA strand to be displaced, confirm the previous results and show that RT alone is able to synthesize in vitro the central DNA flap shown ex vivo, even if the reaction is carried out with an apparent low processivity.

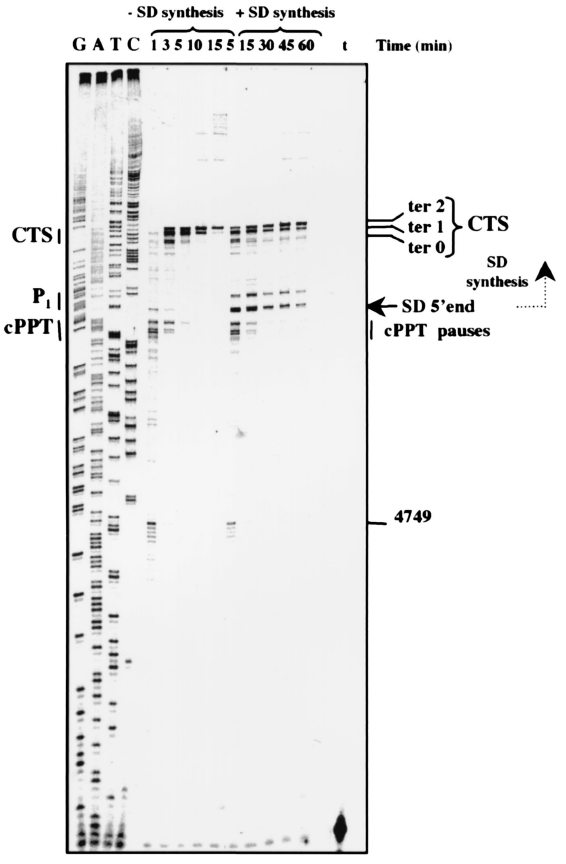

FIG. 3. Comparison of normal DNA synthesis versus SD synthesis along the minus-strand HIV-1 central DNA catalyzed by HIV-1 RT. 5′ ^{33}P-labeled P_0 primer was annealed to pBS-SK(+)–cPPT-CTS to analyze normal synthesis. For the SD reaction unlabeled primer P_1, located 134 nt downstream of P_0, was annealed in addition. A preincubated solution of RT (20 nM) and hybrid (9 nM) were mixed with all four dNTPs (100 μM) to start the reaction. The times of reaction are indicated. Lane t is a control without dNTPs. Lanes G, A, T, and C show a sequencing reaction of the central plus-strand DNA with the corresponding nucleotides using Sequenase and labeled P_0 primer. The conditions of the polymerase reaction, electrophoresis, and visualization are given in Materials and Methods.

SD synthesis is more efficient in the presence of NCp or gp32 protein but still terminates at the CTS sequence generating the central flap. We have analyzed the effect of different viral and SSB proteins during the elongation experiments. These proteins were chosen because of their known properties to be associated with the RT or their positive effect on SD synthesis. The NCp was carefully tested because it is referred as an RT auxiliary compound during the course of reverse transcription, and it transiently behaves like a helix-destabilizing protein (18). SSB proteins such as the human RPA, *E. coli* SSB, and the T4 gene 32 protein (gp32), generally known to promote the strand displacement process (2), were also examined, as well as integrase and viral protein R (Vpr), proposed to be part of the HIV-1 preintegration complex (13). A comparison between these proteins showed that only NCp and gp32 have a noticeable positive effect (data not shown for the other checked proteins). The patterns of pauses obtained in the presence of gp32 and NCp were similar (Fig. 4). The

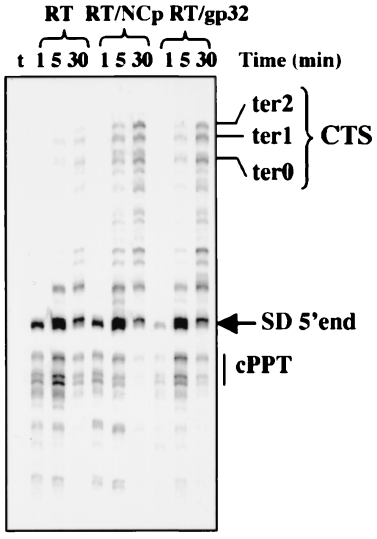

FIG. 4. Effect of NCp and gp32 on the kinetics of SD synthesis. Extension from labeled P_0 primer in combination with unlabeled primer P_1 was performed with a limited amount of RT (6.6 nM) in the presence of NCp (3 μM) or gp32 (3 μM). The concentration of the annealed primer P_0 was 9 nM. Lane t is a control without dNTPs. Products were analyzed as described in Materials and Methods.

applied concentrations of NCp or gp32 were in a range classically used to cover the DNA molecules with protein (one molecule for 10 nt). With RT alone and in limiting amounts (6.6 nM), very few products bypassed the initiation site of SD synthesis (i.e., the 5′ end of P_1 primer), even with incubation times of 30 min. On the other hand, in the presence of NCp or gp32 the amount of longer products increased significantly within an enlarged distribution of the products from the 5′ end of P_1 primer to the ter2 site. The only difference between the effect of NCp and the gp32 is the faster disappearance of pauses within the cPPT when the NCp is used.

To determine the concentration of NCp required for maximal enhancement of SD synthesis, an assay was performed with an RT concentration of 16.6 nM, a hybrid concentration of 9 nM, a 30 μM concentration of nucleotides, and increasing amounts of NCp (from 0.75 to 3 μM, corresponding to one NCp molecule per 40 to one per 2.5 nt) (Fig. 5A). After 10 min in the absence of NCp, the products accumulated at the pausing sites described in the upper section: position +4749, cPPT, and the SD 5′ end, showing the most dramatic effect. Only a very few products were extended up to the CTS. After 50 min, most of the products were extended to the CTS. Adding increasing concentrations of NCp to the reaction led to a steady increase in the length of the DNA products toward the CTS. The cPPT pausing site disappeared rapidly, whereas to suppress the pausing at the SD 5′ end required higher concentrations (one NCp for 5 nt). For all products to terminate at ter0, ter1, and ter2 after 50 min of incubation, an NCp ratio of 1 per 2.5 nt was necessary. At the two higher concentrations of NCp applied, only small amounts of elongated primers up to the cPPT-CTS region were found, whereas the majority of the primers were observed to migrate as free primers in the electrophoresis. This presence of nonextended primers was likely due to an inaccessibility of the primers for RT (8) and/or a disannealing induced by the known destabilizing property of the NCp (47). However, all of the products generated at these concentrations of NCp reached the CTS zone. This clearly demonstrates that NCp increases the processivity of RT during SD synthesis in the cPPT-CTS window. For normal DNA synthesis in this region (i.e., no SD synthesis), similar results were obtained (data not shown).

In order to evaluate more closely the impact of NCp on the RT-directed synthesis, elongation was performed under strand displacement conditions with increasing concentrations of RT (4 to 56 nM) in the absence or presence of NCp (6 μM, one molecule per 6 nt), using a hybrid concentration of 9 nM and incubation times of 10 and 50 min (Fig. 5B). At the lowest RT concentration (4 nM) in the absence of NCp, only very few primers were elongated. At the next higher RT concentrations (8 and 16.4 nM) still without NCp, there were a few more primers elongated with the characteristic pausing sites (4749 and cPPT), while few products reached the CTS after 50 min. In the presence of NCp, no synthesis could be obtained for the lowest concentration of RT (4 nM). When increasing the RT concentration to 28 or 56 nM, some DNA synthesis was observed in the presence of NCp. However, according to the results shown above (Fig. 5B) with high concentrations of NCp, while the majority of primers were not extended, all of the extended ones reached the cPPT-CTS region. With a RT concentration of 28 nM and an incubation time of 50 min, most of the products reached a position between the cPPT and CTS sites without NCp and the ter1-ter2 pausing site with NCp. In the presence of NCp, the efficiency of RT to overrun the pausing sites was increased for both normal synthesis (upstream P_1) and SD synthesis (downstream P_1). Independent of NCp presence, few products were observed to pause at sites downstream of the CTS site at the highest RT concentrations used here. Inhibition of the synthesis observed at a low RT concentration in the presence of NCp could be again explained by the removal of the primer actively from the template by NCp and/or by an inaccessibility of the primers for RT, suggesting a competition for binding between RT and NCp. This effect was obtained for an RT range from 4 to 16.4 nM, with a 9 nM concentration of hybrid (stoichiometric with RT concentration) and an NCp concentration of 5 μM, typically used to cover the DNA (one NCp per 10 nt). It could be circumvented by applying an RT concentration of 28 nM, corresponding to an RT/NCp ratio of 1/150. This defines the minimal RT/NCp ratio necessary to allow initiation of DNA synthesis. This value is quite a bit lower than the situation in the virions, which is about one molecule of RT per 20 molecules of NCp (46).

cPPT RNA primer: an additional barrier for the generation of the central flap. In vivo, the situation is obviously more complex with the cPPT primer consisting of RNA. The generation of this RNA primer by the RNase H activity during negative-strand DNA synthesis has been shown experimentally for HIV and equine infectious anemia virus (27, 44). Therefore the 5′ nucleotide of the P_1 primer should be next to the 3′ nucleotide of the cPPT primer (4). Further, according to studies on the elongation from the 3′ PPT, it can be proposed that after priming from the cPPT RNA and incorporation of several nucleotides, the newly generated RNA-DNA chimera is cleaved by the RNase H activity, and the cPPT primer stays annealed to the DNA template (17, 40). Up to this stage, we

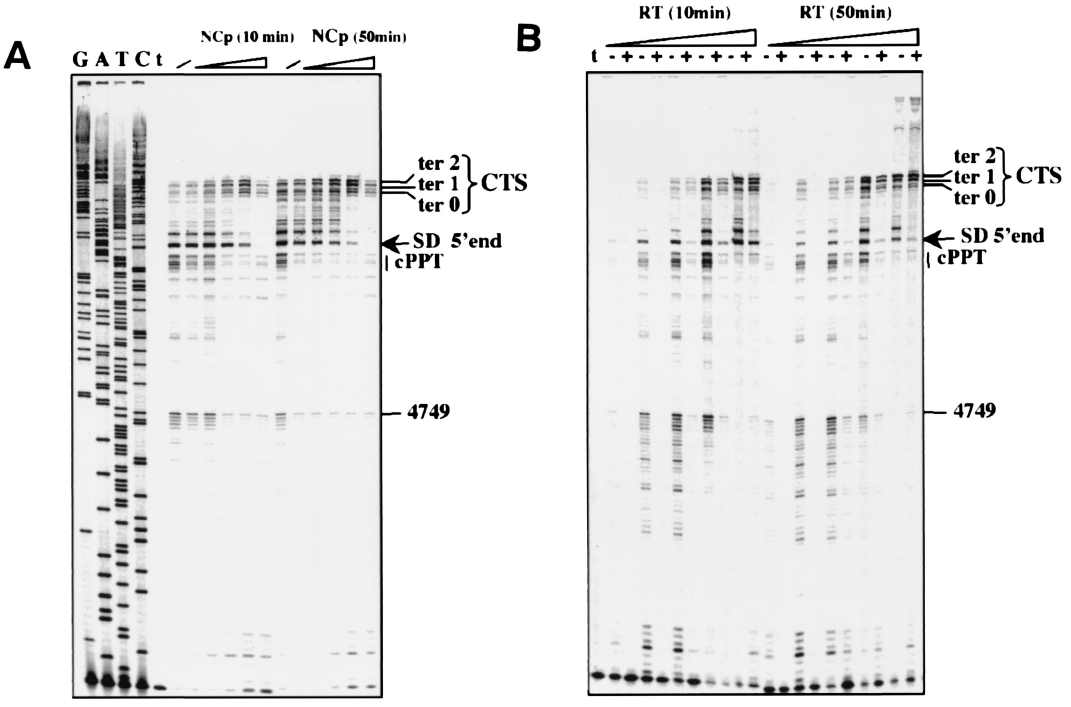

FIG. 5. Dependence of the SD synthesis on the NCp and RT concentrations. (A) Products of SD synthesis with a fixed concentration of RT (16.6 nM) and increasing amounts of NCp (0.75, 1.5, 3, 6, and 12 μM). (B) Products for SD synthesis with increasing amounts of RT (4, 8, 16.4, 28, and 56 nM) and a fixed concentration of NCp (4.4 μM). In both cases, the reactions were performed for 10 and 50 min, respectively. The concentration of the annealed primer P_0 was 9 nM. Lane t is a control without dNTPs. Products were analyzed as described in Materials and Methods.

deliberately neglected this experimental complication circumstance to fully focus on the synthesis of the final product of reverse transcription (i.e., the central flap).

However, since it is not known whether this RNA primer is still present during SD synthesis in vivo, we performed experiments with a labeled P_0 primer in the presence of the cPPT RNA (Fig. 6). Without the cPPT RNA primer, a weak pausing at the cPPT site was observed in the first minute, as well as other pausing events up to the CTS site. After 5 min of incubation the products were located only at the ter1 and ter2 sites, and after 30 min they started to accumulate at the ter2 site, with some products elongated up to sites downstream of the CTS. With the cPPT RNA primer, the three bands typically found for pausing at the cPPT were observed within 1 min as described above (Fig. 3 to 5). This pattern did not change much with additional incubation times up to 30 min, although a few products reached the ter1 and ter2 sites. Therefore, initiation of SD synthesis was clearly less efficient with the RNA primer. In contrast, the pausing pattern obtained with the downstream P_1 primer appears quite different. Already after 5 min, strong pausing was visible at the SD 5′ end and the ter1 and ter2 sites. Further incubation for up to 30 min triggered the cPPT pausing site to disappear and the pausing at the SD 5′ end to be strongly reduced. When the same kind of experiment was performed with both the P_1 and the cPPT RNA primer annealed, the two types of pausing events (cPPT and SD 5′ end) were found again, the stronger one being at the cPPT level. These results show that bypassing the pause site at the SD 5′ end is easier than at the cPPT site with an annealed RNA primer: the cPPT RNA staying on the template represents a very strong barrier in an SD synthesis context. Furthermore, these results also suggest that DNA and RNA displacements are not equivalent. Experiments with the cPPT primer consisting of DNA

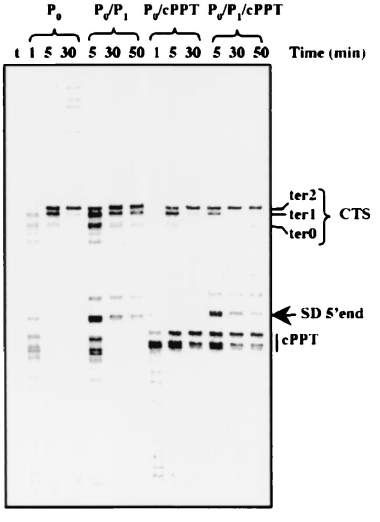

FIG. 6. Comparison of P_0 primed DNA synthesis with or without the P_1 primer, the cPPT RNA, or a combination of both. The concentrations of the labeled P_0 primer and RT were 9 and 16.4 nM, respectively. Lane t is a control without dNTPs. The conditions of electrophoresis and visualization are as described in Materials and Methods.

instead of the RNA revealed a fast bypassing of the pause site at the cPPT level (data not shown). As an RNA-binding protein, NCp might play a role in this context. In order to analyze its effect on RNA displacement, compared to gp32, these proteins were added to the reaction. NCp was partially efficient to assist this reaction, while gp32 was not (data not shown).

After one round of elongation, HIV-1 RT-catalyzed SD synthesis is not effective along the circular template to perform a rolling circle but is effective to produce the central flap. In order to study the SD synthesis in conditions closer to the in vivo situation, we have analyzed complete DNA synthesis along our circular ssDNA template with only one primer annealed: P_1 or P_2 (H_1 or H_2 hybrids). Here, the first round of DNA synthesis is normal, whereas the following rounds require SD synthesis. With an efficient SD synthesis, the reaction resembles the situation of rolling circle replication (2). Observing the polymerization properties of HIV-1 RT in such a reaction allows us (i) to easily assess the efficiency of RT in SD synthesis anywhere along the template; (ii) to directly study both normal synthesis and SD synthesis for a DNA length closer to in vivo PPT-primed plus-strand DNA segments; and (iii) to devise some more sophisticated in vitro experiments in order to study the functional relationships between HIV-1 plus-strand synthesis, central flap formation, and the assembly of HIV-1 preintegration complexes.

Complete DNA synthesis requires 3,335 nt to be incorporated for the first round. This can be analyzed, after quenching the reaction, by agarose gel electrophoresis of the DNA products. The successive conversions from circular ssDNA to dsDNA result in a consecutive gel shift of the products (Fig. 7A, H_1 and H_2, from 0 to 20). Using a 20-fold excess of RT over the annealed primer (100 versus 5 nM) at 37°C, a full circle is observed within 20 min regardless of the starting positions P_1 and P_2, respectively. Incubation for another 40 min did not change the electrophoretic properties of H_1. A slight smear could be observed for H_2 (Fig. 7A, H1 and H2, from 20 to 60). Discrete bands were obtained for H_1 after 60 min of incubation with RT, followed by digestion with *Dra*III or *Alw*nI, while the smear was markedly increased for H_2 linear products (Fig. 7A, H1 and H2, a and b). A double digestion of the products with these two enzymes under the same conditions generated two discrete bands for H_1, whereas the faster band in case of H_2 disappeared completely, being replaced by a slow-migrating smear(Fig. 7A, H1 and H2, c). As shown in Fig. 2, the faster band contains the P_2 sequence (shorter fragment) and the slower band contains the P_1 sequence (larger fragment). These data demonstrate that SD synthesis indeed occurs after one round of elongation along the circular template. In the case of the H_1 hybrid, the extended P_1 primer was displaced and the reaction stopped at the CTS site (as shown above; see also Fig. 3 and 5), producing the central flap. However, the displaced strand is too short (99 nt at maximum) to reduce the mobility of the dsDNA. The H_2 hybrid progressed gradually after initiation from the P_2 position, generating a growing strand displacement shifting the dsDNA in a very heterogeneous manner. This tail did not reach the CTS since it stops before without any discrete termination. In case of a discrete termination event, one would have obtained a discrete band shift and not a smeary shift. However, the limited smearing effect indicates that tail extension is easily blocked nonspecifically by some unknown mechanism (see below).

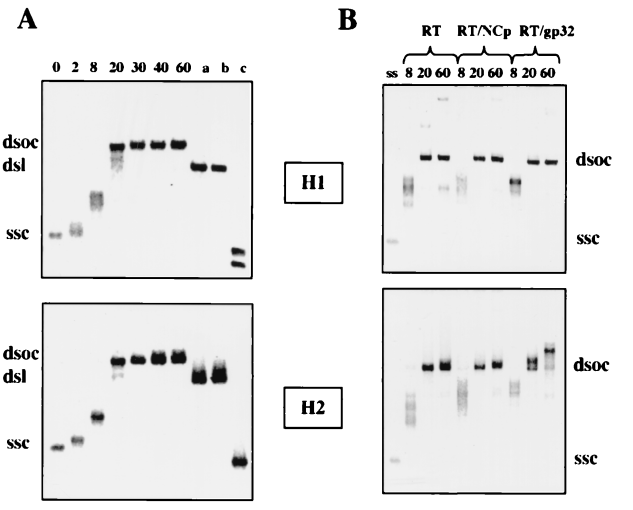

FIG. 7. DNA synthesis along the circular ssDNA template with the primers P_1 or P_2 annealed to the template. The corresponding hybrids are named H_1 and H_2. (A) The kinetics of the reaction with HIV-1 RT (100 nM) are shown for each hybrid (5 nM) from 0 to 60 min (see top of the gel): DNA products were shifted gradually from the circular ssDNA (ssc) to the open circular dsDNA (dsoc). After 60 min, *Dra*III and *Alw*NI (see Fig. 2) were added to the mixture separately (a and b) or together (c) for another 30 min. Simple digestions linearized the circular dsDNA (dsl), while the double digestion is supposed to generate two fragments (P_1 and P_2 sequences are located within the larger and the shorter fragment, respectively). (B) Comparison of the kinetics (8, 20, and 60 min) of DNA synthesis is shown on agarose gels with the same hybrids H_1 and H_2 (H1 and H2, 5 nM each) with RT alone (150 nM), RT (150 nM) plus NCp (3 μM), and RT (150 nM) plus gp32 (3 μM). The ss lane contains a circular ssDNA (ssc) as a control. After preformation of the RT-DNA complexes for 2 min, NCp and gp32 were added to the mixtures together with the dNTPs. Reactions were stopped with 1% LDS and 50 mM EDTA. The conditions of the reactions, electrophoresis, and fluorescent visualization are given in Materials and Methods. SYBR Green I fluorescence is enhanced as the base pair contents increase within the DNA circles.

Since NCp and gp32 were shown to be effective in promoting SD synthesis within the P_1-CTS region, DNA synthesis along the circular template was carried out in the presence of these proteins using both hybrids H_1 and H_2 (Fig. 7B). The first set of experiments was performed for 20 min. NCp, as well as gp32, was shown to slightly speed up this process (Fig. 7B, shifted band after 8 min of incubation). From 20 to 60 min of incubation, the dsDNA bands in case of H_1 remain the same regardless of whether NCp or gp32 is added or not. However, two minor but discrete, slower-migrating bands appeared. This is most likely due to recombination events caused by SD synthesis (see also Fig. 10 and the next section). For H_2, the situation is different in respect to the auxiliary proteins. A slight smear was obtained for RT alone and RT with NCp added to the reaction. However, with gp32 the DNA products progressively shifted to more discrete bands, indicating SD synthesis to be more efficient in this case (already after 20 min). None of the other DNA-binding proteins investigated with this assay gave such a result (data not shown), though human RP-A and *E. coli* SSB have some effect, as already shown by others for SD synthesis within the LTR (1, 14).

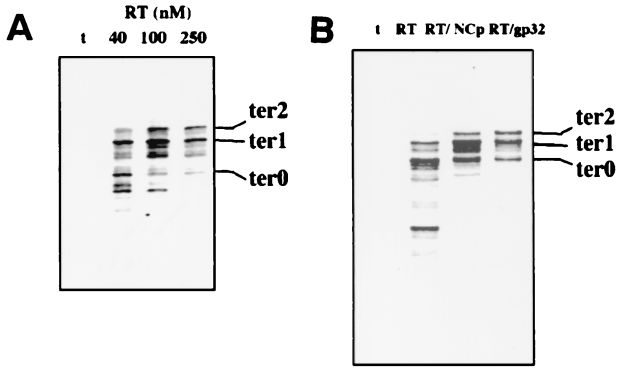

FIG. 8. Analysis of the exact position of 3′ end of the nascent strand with H_1 hybrid after 60 min of DNA synthesis. (A and B) Increasing concentrations of RT (40, 100, or 250 nM) (A) or RT, RT-NCp, or RT-gp32 (RT, 20 nM; NCp, 2 μM; gp32, 2 μM). DNA produced from H_1 was digested with *Eco*RI and consequently treated with phosphatase, followed by a kinase reaction in the presence of [γ-^{33}P]ATP, and then subjected to electrophoresis in a sequencing gel as indicated in Materials and Methods. With this postlabeling experiment, three labeled DNA strands were generated. The template strand was linearized, and the nascent strand was cut into a long fragment, from P_1 to the *Eco*RI site, and into a short fragment, from the *Eco*RI site to its 3′ end located in the P_1-CTS region due to the incomplete SD synthesis. This fragment migrated in a sequencing gel, when the length of the two others was longer than 3,000 nt. Lane t is a control without dNTPs.

The major goal to be accomplished with this circular DNA synthesis system was to analyze both the RT efficiency to produce the HIV-1 central DNA flap after a 3,335-nt primer extension and to investigate the products of this reaction. Using the H_1 hybrid to generate the central flap after one round of DNA elongation, the agarose gel analysis revealed that SD synthesis was clearly blocked close to its initiation. The experiments, shown above using two primers, were done with the P_0 primer as the labeled primer (compare Fig. 3 to 6), where the 5′ end of this primer matched with the 5′ end of the *Eco*RI site in the nascent strand. Thus, in order to analyze the pausing profile of the nascent strand, DNAs were cut by *Eco*RI and subsequently 5′ end labeled with ^{33}P. A particular set of samples was analyzed in such a manner (Fig. 8). The reactions were allowed to proceed for 60 min, applying increasing concentrations of RT (Fig. 8A) or adding either NCp or gp32 at a limiting concentration of RT (Fig. 8B). This resulted in the generation of a central flap within the circular DNA showing a 3′-end distribution of the nascent strand within the CTS site, predominantly in the ter1-ter2 window. This clearly shows that in vitro synthesis of the HIV-1 central DNA flap, which occurs after one round of elongation, follows the same pattern as that described above.

EM gives the opportunity to complete these data by the direct observation of individual DNA molecules at various stages of DNA synthesis, as well as in different experimental conditions. After the reactions were stopped, the products were purified by gel filtration chromatography and visualized in the presence or absence of gp32. This SSB protein is used for EM since, by covering ssDNA, it allows its spreading, leading to a blurred filament (Fig. 9a), thicker than the double-stranded counterpart (Fig. 9b). This allows unambiguous visualization of the single-stranded structure of the flap (Fig. 9b to d), whose length varies according to the hybrids (H_1, H_2) used. H_1 incubated with RT for 60 min resulted in the generation of a major population of dsDNA with a small, homogeneously tailed ssDNA that was no more than 100 nt long (Fig. 9b). Digestion by *Dra*III-*Alw*NI allowed us to confirm the flap position (Fig. 9c). Under the same conditions of incubation, H_2 led to the generation of a major population with a larger, heterogeneous extruded ssDNA with an average length of ca. 400 nt (Fig. 9d). A second minor population was also found, exhibiting an unexpected tailed filament, derived from the flap, which was either double stranded (Fig. 9e) or partially double and single stranded (Fig. 9f). Interpretation of these results is discussed in the next section.

A high level of strand transfer occurs during SD synthesis with RT alone and a 3′-5′ branch migration is highlighted as a possible event during synthesis of the central flap by HIV-1 RT. EM has revealed some atypical products with the H_2 monomeric circular forms: dsDNA circles with an extruded dsDNA (Fig. 9e) or with an extruded dsDNA terminated with a ssDNA loop (Fig. 9f). It showed that an increase in length during SD synthesis favored the occurrence of dsDNA within the tails that may block further DNA elongation, thus explaining the limited smearing shift for the dsDNA products on an agarose gel. Extruded dsDNA means that a direct strand transfer of the nascent strand from its native template to the displaced strand, at the vicinity of the branching site, was followed by a DNA synthesis along the initial displaced strand. Extruded dsDNA terminated with a DNA loop may be explained by a 3′-5′ branch migration displacing the nascent strand, followed by an intra-annealing of its 3′ end with an upstream site generating a ssDNA loop and subsequently by its elongation that can even displace the initial template. These intracircular misalignments within the displaced strands favor some improper DNA elongation and display HIV-1 RT as a degenerating DNA polymerase to perform SD synthesis.

Formation of the central flap with H_1 hybrid was concerned by such degenerating events, but to a lesser extent, presumably because of the smaller size of the displaced strand. On the other hand, two discrete bands appeared with an important shift from the normal circular dsDNA form during the course of DNA synthesis with H_1 hybrid (Fig. 7, H1). Moreover, this event was not abolished but was strongly reduced with the H_2 hybrid. Changing the ratio of template to primer was critical for this effect: as the free template was increased in our hybrid preparation, the amount of shifted band also increased. For a 1:2 ratio instead of 1:4 with H_1 hybrid, the two bands appeared sequentially during the incubation (Fig. 10a; 30 and 60 min), the slowest band being the latest to be produced. EM visualization explained the sequential formation of these products: the first band to appear corresponded to a pair of DNA circles with one dsDNA linked to one ssDNA (ds-ss; Fig. 10a and b), when the second band contained a pair of two linked dsDNA (ds-ds; Fig. 10a and d).

Such a visualization confirmed what the previous results have shown about the efficiency of DNA-to-DNA strand transfer in the course of SD synthesis along the cPPT-CTS site, according to the strand displacement assimilation model (16). Indeed, after one round of DNA elongation and SD synthesis up to the CTS, the nascent strand, which is in competition with

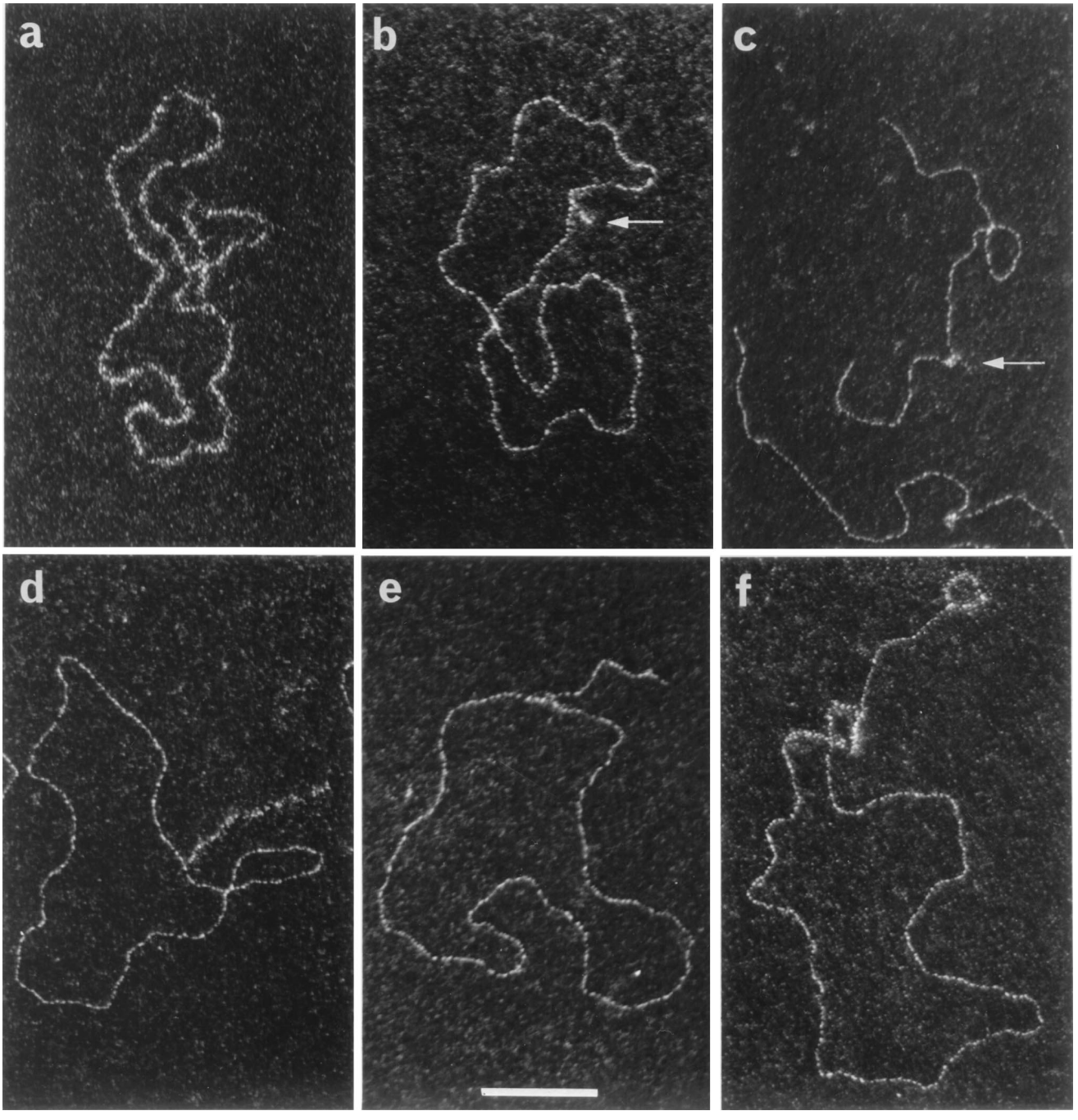

FIG. 9. Electron micrographs of single DNA molecules. Representative circular dsDNA molecules produced after a 60-min incubation by RT are obtained after deposition of the purified DNA products on a carbon film without (e) or with gp32 protein used to coat ssDNA (a, b, c, d, and f). (a) Circular ssDNA molecule covered by gp32. (b to d) Typical circular dsDNA molecules containing a single-stranded flap revealed by gp32, H_1, and H_2, respectively. (c) Localization of the flap within in a linear H_1 dsDNA after *Alw*NI-*Dra*III digestion. (e and f) Less-abundant species of circular dsDNA generated from H_2 with atypical flaps (see Results). Preparations of the samples for EM are as indicated in Materials and Methods. Bar, 100 nm.

the displaced strand, may dissociate from its original template. If a complementary strand is available in the mixture, the nascent strand will reassociate with this template (Fig. 10b) and, thus, will continue its synthesis on the new template (Fig. 10c and d). The strand transfer is done within minutes for a nascent strand concentration of 5 nM and, if free templates are in excess, all of the nascent strands may be transferred (not shown). Therefore, this strong efficiency of strand transfer means that competition between the two overlapping strand strongly favors a 3′-5′ branch migration to dissociate the nascent strand. This may be an important factor for CTS termination in an SD synthesis context. When RT dissociates from

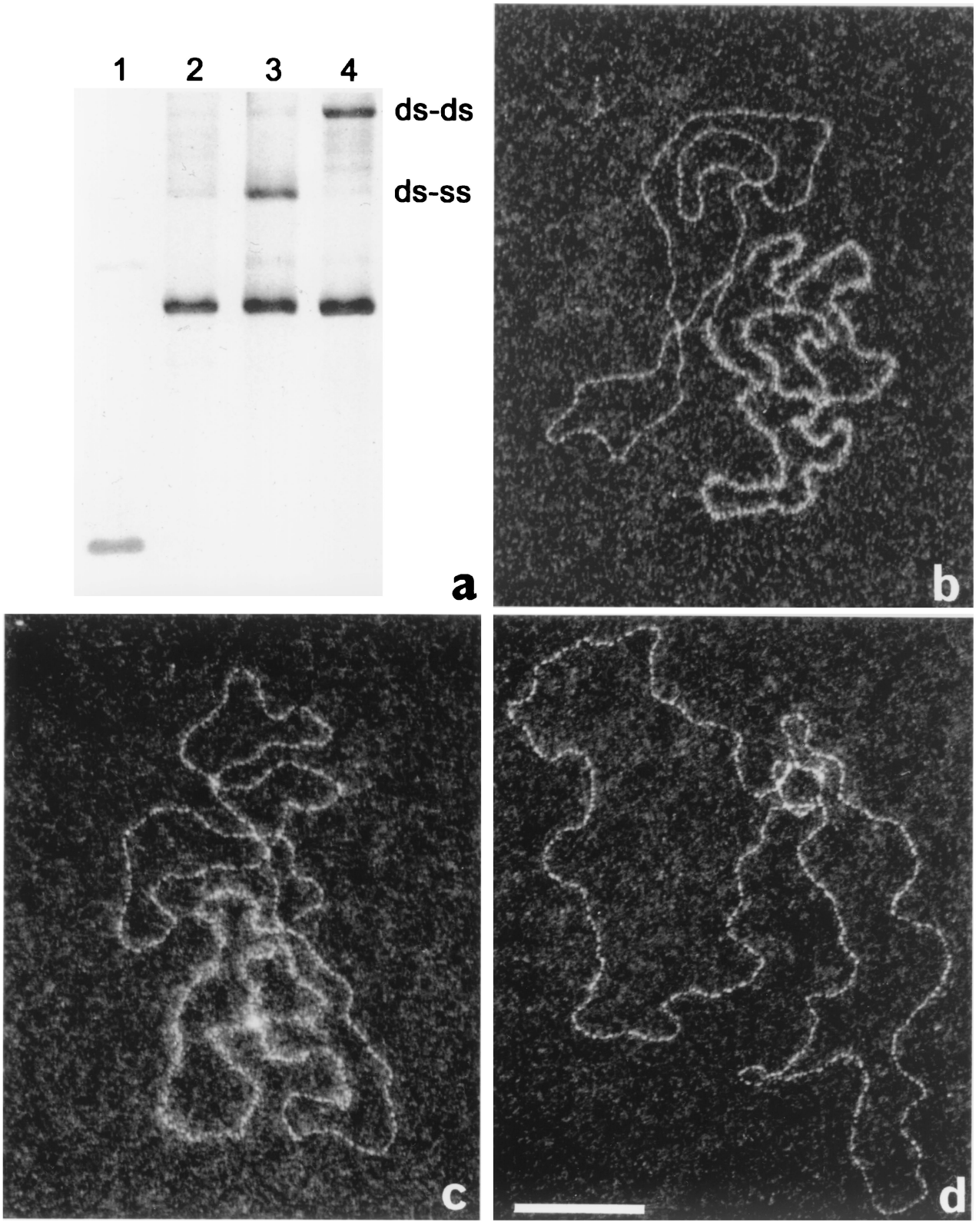

FIG. 10. DNA synthesis, strand transfer, and circular dimers. DNA synthesis was carried out with the H_1 hybrid for 0, 15, 30, and 60 min (lanes 1 to 4) with a template/P_1 primer ratio of 1:2 (RT, 150 nM; H_1, 5 nM). Products of the reaction were observed by electrophoresis on an agarose gel (a) and by EM in the presence of gp32 protein (b to d). The slowest and latest band (ds-ds) to appear in the gel correlates to a population of DNA on the EM grid, which is represented here by this pair of linked circular dsDNA (d). The intermediate band (ds-ss) correlates to a population of DNA which represents two linked individual species: each of these molecules is composed of one circular ssDNA linked to one circular dsDNA (b). Micrograph c illustrates the elongation along the second circle (transition between images in panels b and d). The conditions of reactions, electrophoresis, fluorescent visualization, and preparations of the samples for EM are given in Materials and Methods. SYBR Green I is much less sensitive for ssDNA than for dsDNA: for incubation times of less than 15 min, the amount of nonprimed ssDNA is below the detection limit. Bar, 100 nm.

one of the ter sites, especially in ter2, a concomitant 3′-5′ branch migration should occur and definitively prevent further elongation. This strand transfer also occurred with the H_2 hybrid, but to a lesser extent that suggested that the P_1-CTS was especially sensitive to 3′-5′ branch migration, as already proposed (16). More experiments are required to better understand this putative relationship between branch migration and CTS native termination. While the related recombination should be avoided in vivo since a DNA acceptor seems to fail at this step of proviral DNA synthesis, it suggests that the central flap should be considered as a dynamic structure at least at the time of its synthesis. The impact of NCp, gp32, or any other protein(s) still should be evaluated in view of such a potentially degenerative process which terminates HIV-1 reverse transcription with the central flap and the two LTR sequences (with ~640 nt to be displaced).

DISCUSSION

To study the HIV-1 central flap at the molecular level, we performed experiments to reconstitute the sequential steps of the central termination of plus-strand DNA synthesis in vitro. Our results represent the first example of a complete HIV-1 central DNA flap produced in vitro by the homologous RT. The reaction is enhanced by HIV-1 NCp. Interestingly, gp32 was shown to be more effective in promoting long-range SD synthesis. Otherwise, the high level of strand transfer observed during SD synthesis along the cPPT-CTS site reveals an efficient 3′-5′ branch migration within the flap. The present data bear on the consequences of HIV-1 central DNA flap synthesis on the molecular mechanisms of the poorly understood transition from RTCs to PICs, which are competent for nuclear import and integration of the HIV-1 DNA.

The mechanism of RT pausing has been investigated in detail for the cPPT-CTS region, especially the CTS-associated ter0, ter1, and ter2 positions (6, 26, 28, 29, 44). These pausing events, in the context of normal or SD synthesis, strongly decrease the global RT processivity. The CTS double helix was shown to locally adopt a certain conformation (compression of the minor groove) that promotes dissociation of RT (29, 44). We have extended these previous studies to the entire cPPT-CTS sequence with a highly purified template in order to generate the central DNA flap, and we have compared the SD synthesis with simple elongation. The pausing pattern is similar with or without SD. However, the SD reaction slows down the HIV-1 RT-catalyzed DNA synthesis. Our results showed a 10-fold reduction in the overall rate of reaction in a complete SD synthesis context to reach the ter1 and ter2 sites (Fig. 3). These data are concordant with previous results obtained with HIV-1 RT (14, 20) and the MMLV RT (49) in the LTR-related SD synthesis, even if the MMLV RT appeared to be more potent in a long-range SD synthesis (49, 50). Otherwise, SD synthesis with the cPPT RNA to be displaced appeared to be a very slow process (Fig. 6), as already shown for RNA-SD synthesis with HIV-1 RT (15) and with MMLV RT (25).

Various interactions between RT and NCp have been proposed during the crucial steps of HIV-1 reverse transcription (18). Our results indicate that both proteins are required for the final step of flap synthesis to be efficient. This requires in vitro the NCp concentration to be sufficient to cover completely the DNA. In addition, the concentration of RT must be high to overcome the poor RT processivity along a DNA template, especially for SD synthesis (determined here with a minimum RT/NCp ratio of 1 to 150). The discrete pausing of RT observed along the HIV-1 DNA minus-strand template was significantly reduced by NCp during both simple elongation and SD synthesis, while gp32 preferentially decreased the pausing during SD synthesis (Fig. 4 and 7). Thus, it seems that the helix-destabilizing activity of NCp is not the driving force to promote SD synthesis. When the DNA synthesis products in the presence of RT and NCp are directly visualized by EM without purification, it is apparent that they are made within DNA-NCp condensates (unpublished results). This nucleic acid condensing activity is an important property of NCp (32, 47). Therefore, the interaction between NCp and RT may hold RT in the vicinity of the substrate; even so, RT dissociates from the DNA. This might be especially important within a cellular environment to stabilize the RTC (9, 33). Concerning the NCp chaperone activity on nucleic acids, it has been proposed that the helix-destabilizing activity is counterbalanced by its annealing activity (41). This could explain the limited effect of NCp to promote long-range SD synthesis (Fig. 7), while it should be quite effective for promoting a specific structural arrangement of the central DNA flap. Besides, NCp did not assist RT in bypassing the ter2 site, which is only overrun in case of a large excess of RT (Fig. 5 and 8). This suggests an additional barrier in SD synthesis to further lock elongation after RT dissociation from the ter1 and ter2 sites, which should be the potent branch migration that easily exchanges the nascent strand with the displaced one (Fig. 10).

Looking at the last steps of plus-strand DNA synthesis leads to consider together the two HIV-1 termination steps: at the end (LTR duplication) and at the center (central flap). Nevertheless, how the plus-strand DNA synthesis is coordinated to lead to the termination steps and consequently to the proviral DNA is still an open question. The answer to this question is likely to be crucial to our understanding of the transition between RTCs and PICs. At the level of LTR duplication, the efficiency and fidelity of this process has been already discussed. The SD synthesis to duplicate the LTRs may directly represent one important barrier to the PIC's maturation. During the course of our experiments with RT alone, SD synthesis appeared to easily generate some intramolecular recombination (Fig. 10), confirming previous results (14). Furthermore, we observed a better efficiency with gp32 compared to NCp (Fig. 7) or to the human SSB RP-A (not shown) to promote elongation during SD synthesis. This suggests that LTR duplication would require some other component than NCp, i.e., another viral protein or some cellular SSB protein, which may be more potent or more accessible than RP-A, as already proposed by others (1, 14). The occurrence of a second initiation of plus-strand DNA synthesis, as the HIV-1 cPPT-directed one, has also been proposed to assist the LTR duplication, since the downstream plus-strand elongation reaches the LTR locus faster. This would provide the opportunity for two converging RTs to engage SD synthesis within the LTR (Fig. 1) (49). This second initiation step also generates two sliding complexes instead of one along the minus-DNA template and, thus, changes the transition profile between ssDNA and dsDNA during the synthesis along the genome (Fig. 1). Sliding

complexes and ss-ds transition profiles could be major factors for driving the change in the distribution of proteins linked to the HIV-1 genome. Apart from the synthesis of the central DNA flap and of the two LTR ends, such a behavior could lead to a better-adapted assembly for an active HIV-1 PIC, i.e., to optimize the most active architecture between the proviral DNA, the integrase, and the other PIC-relevant proteins.

Coming back to the central flap, this structure could function as a protein catcher because of its single-stranded nature, the only significant single strand left after completion of reverse transcription. This might play a role in binding specifically certain proteins to the RTC, a step which could promote the transition from RTC to a functional PIC. If the HIV-1 central DNA flap retains some direct and specific interactions, then the primary sequence stretching from the cPPT to the CTS should contain some specific conformational elements, as already shown within the CTS minor groove (28, 29). On the other hand, the flap, which requires an adapted form to resist the intracellular repair process, especially the flap nuclease FEN-1, has been shown to be maintained up to some intranuclear integration (6). Indeed, the FEN-1 enzyme has been shown to remove the 5′ tail of the HIV-1 central DNA flap branched to a nonanalogous duplex DNA, where the strand exchange is avoided (42). In front of this, the branch migration revealed here (Fig. 9 or 10) and the resulting flip-flop fluctuation may constitute an intermediary step to favor some selective secondary structure. Alternatively, at the time RT dissociates from the ter1-ter2 locus, the flap may interact directly with one of the PIC components, avoiding some backward branch migration. Apart from the NCp, integrase is then a possible ligand, since the flap mimics an intermediary form in the integrative pathway (7).

The HIV-1 central initiation-termination strategy of DNA synthesis has been previously shown to favor the HIV-1 life cycle (5, 6). Recently, this strategy has been experimentally shown to optimize the nuclear import of PICs for both HIV-1 and HIV-derived vectors (12, 53). This nuclear import (or intranuclear targeting) effect may be gained as a consequence of the double initiation-termination strategy on the PIC assembly, while it clearly involves the nucleophilic properties of some of their components (13). With regard to simple retroviruses (e.g., avian myeloblastosis virus and MMLV), which appear not to possess an active mode of nuclear import, the differences between the related PICs can be emphasized. The Vpr and Vpx proteins and the central DNA flap, lentivirus-specific components, arise as attractive elements to promote the PIC's nuclear import (13, 45). Concerning the flap, its genetic suppression showed a marked decrease in nuclear import: it is proposed to be engaged in direct interactions with the cellular machinery for nuclear import (12, 53). Soluble cargos and/or translocation factors within the nuclear pore complexes are discussed in this context (53). Furthermore, interactions of the flap with DNA and RNA binding proteins possessing nucleophilic properties are also proposed (53).

Finally, it should be addressed why especially lentivirus have developed such a strategy for a central DNA flap synthesis. This would, for example, imply comparing the final steps of reverse transcription, the RTC-to-PIC transition, and the nuclear import of the HIV-1 with that of other lentiviruses. This could lead to a better understanding of both the fundamental (nuclear targeting of lentivirus) and the pharmacological (anti-HIV-1 as well as gene delivery) perspectives of such an unexpected phenomenon. In this regard, the experimental system that we have developed allows us to perform in vitro experiments with the central DNA flap as the main actor in order to analyze both its structure(s) and its fluctuations, to delineate its binding to the large set of its putative protein partners, to approach its impact in the RTC-to-PIC transition, and to check its efficiency in the DNA, or DNA-protein(s), nuclear import.

ACKNOWLEDGMENTS

We thank Lou Henderson and Rob Gorelick for graciously providing HIV-1 NC protein and Valérie Barbe and Michel Lacasa for helping to start the preparation of our ssDNA. We are indebted to Pierre Charneau and Henri Buc for initial support, to Malcolm Buckle and Bianca Sclavi for helpful comments, and to Olivier Schwartz and Caroline Petit for reading drafts of the manuscript.

This work was supported by grants from the Agence Nationale de Recherche sur le SIDA (ANRS). L.H. is the recipient of a fellowship from ANRS. G.M. is Assistant Professor at the Université Pierre et Marie Curie (Paris VI).

REFERENCES

1. **Amacker, M., M. Hottiger, R. Mossi, and U. Hubscher.** 1997. HIV-1 nucleocapsid protein and replication protein A influence the strand displacement DNA synthesis of lentiviral reverse transcriptase. AIDS Res. Hum. Retrovir. **11:**534–536.
2. **Baker, T. A., and A. Kornberg.** 1992. DNA replication, 2nd ed. W. H. Freeman and Co., New York, N.Y.
3. **Cameron, C. E., M. Ghosh, S. F. Le Grice, and S. J. Benkovic.** 1997. Mutations in HIV reverse transcriptase which alter RNase H activity and decrease strand transfer efficiency are suppressed by HIV nucleocapsid protein. Proc. Natl. Acad. Sci. USA **94:**6700–6705.
4. **Charneau, P., and F. Clavel.** 1991. A single-stranded gap in human immunodeficiency virus unintegrated linear DNA defined by a central copy of the polypurine tract. J. Virol. **65:**2415–2421.
5. **Charneau, P., M. Alizon, and F. Clavel.** 1992. A second origin of DNA plus-strand synthesis is required for optimal human immunodeficiency virus replication. J. Virol. **66:**2814–2820.
6. **Charneau, P., G. Mirambeau, P. Roux, S. Paulous, H. Buc, and F. Clavel.** 1994. HIV-1 reverse transcription. A termination step at the center of the genome. J. Mol. Biol. **241:**651–662.
7. **Chow, S. A., K. A. Vincent, V. Ellison, and P. O. Brown.** 1992. Reversal of integration and DNA splicing mediated by integrase of human immunodeficiency virus. Science **255:**723–726.
8. **Driscoll, M. D., and S. H. Hughes.** 2000. Human immunodeficiency virus type 1 nucleocapsid protein can prevent self-priming of minus-strand strong stop DNA by promoting the annealing of short oligonucleotides to hairpin sequences. J. Virol. **74:**8785–8792.
9. **Druillennec, S., A. Caneparo, H. de Rocquigny, and B. P. Roques.** 1999. Evidence of interactions between the nucleocapsid protein NCp7 and the reverse transcriptase of HIV-1. J. Biol. Chem. **274:**11283– 11288.
10. **Dubochet, J., M. Ducommun, M. Zollinger, and E. Kellenberger.** 1971. A new preparation method for dark-field electron microscopy of biomacromolecules. J. Ultrastruct. Res. **35:**147–167.
11. **Fassati, A., and S. P. Goff.** 1999. Characterization of intracellular reverse transcription complexes of Moloney murine leukemia virus. J. Virol. **73:** 8919–8925.
12. **Follenzi, A., L. E. Ailles, S. Bakovic, M. Geuna, and L. Naldini.** 2000. Gene transfer by lentiviral vectors is limited by nuclear translocation and rescued by HIV-1 pol sequences. Nat. Genet. **25:**217–222.
13. **Fouchier, R. A., and M. H. Malim.** 1999. Nuclear import of human immunodeficiency virus type-1 preintegration complexes. Adv. Virus Res. **52:**275–299.
14. **Fuentes, G. M., L. Rodriguez-Rodriguez, C. Palaniappan, P. J. Fay, and R. A. Bambara.** 1996. Strand displacement synthesis of the long terminal repeats by HIV reverse transcriptase. J. Biol. Chem. **271:**1966–1971.
15. **Fuentes, G. M., P. J. Fay, and R. A. Bambara.** 1996. Relationship between plus strand DNA synthesis and removal of dowstream segments of RNA by human immunodeficiency virus, murine leukemia virus and avian myeloblastoma virus reverse transcriptases. Nucleic Acids Res. **24:**1719–1726.
16. **Fuentes, G. M., C. Palaniappan, P. J. Fay, and R. A. Bambara.** 1996. Strand displacement synthesis in the central polypurine tract region of HIV-1 promotes DNA to DNA strand transfer recombination. J. Biol. Chem. **271:** 29605–29611.
17. **Götte, M., G. Maier, A. M. Onori, L. Cellai, M. A. Wainberg, and H.**

Heumann. 1999. Temporal coordination between initiation of HIV positive-strand DNA synthesis and primer removal. J. Biol. Chem. **274:**11159–11169.
18. **Götte, M, X. Li, and M. A. Wainberg.** 1999. HIV-1 reverse transcription: a brief overview focused on structure-function relationships among molecules involved in initiation of the reaction. Arch. Biochem. Biophys. **365:**199–210.
19. **Guo, J., L. E. Henderson, J. Bess, B. Kane, and J. G. Levin.** 1997. Human immunodeficiency virus type 1 nucleocapsid protein promotes efficient strand transfer and specific viral DNA synthesis by inhibiting TAR-dependent self-priming from minus-strand strong-stop DNA. J. Virol. **71:**5178–5188.
20. **Hottiger, M., V. N. Podust, R. L. Thimmig, C. McHenry, and U. J. Hübscher.** 1994. Strand displacement activity of the human immunodeficiency virus type 1 reverse transcriptase heterodimer and its individual subunits. J. Biol. Chem. **269:**986–991.
21. **Hungnes, O., E. Tjotta, and B. Grinde.** 1991. The plus strand is discontinuous in a subpopulation of unintegrated HIV-1 DNA. Arch. Virol. **116:**133–141.
22. **Hungnes, O., E. Tjotta, and B. Grinde.** 1992. Mutations in the central polypurine tract of HIV-1 result in delayed replication. Virology **190:**440–442.
23. **Ji, X., G. J. Klarmann, and B. D. Preston.** 1996. Effect of human immunodeficiency virus type 1 (HIV-1) nucleocapsid protein on HIV-1 reverse transcriptase activity *in vitro*. Biochemistry **35:**132–143.
24. **Karageorgos L, P. Li, and C. J. Burrell.** 1993. Characterization of HIV replication complexes early after cell-to-cell infection. AIDS Res. Hum. Retrovir. **9:**817–823.
25. **Kelleher, C. D., and J. J. Champoux.** 1998. Characterization of RNA strand displacement synthesis by Moloney murine leukemia virus reverse transcriptase. J. Biol. Chem. **273:**9976–9986.
26. **Klarmann, G. J., C. A. Schauber, and B. D. Preston.** 1993. Template-directed pausing of DNA synthesis by HIV-1 reverse transcriptase during polymerization of HIV-1 sequences *in vitro*. J. Biol. Chem. **268:**9793–9802.
27. **Klarmann, G. J., H. Yu, X. Chen, J. P. Dougherty, and B. D. Preston.** 1997. Discontinuous plus-strand DNA synthesis in human immunodeficiency virus type 1-infected cells and in a partially reconstituted cell-free system. J. Virol. **71:**9259–9269.
28. **Lavigne, M., P. Roux, H. Buc, and F. Schaeffer.** 1997. DNA curvature controls termination of plus strand DNA synthesis at the centre of HIV-1 genome. J. Mol. Biol. **266:**507–524.
29. **Lavigne, M., and H. Buc.** 1999. Compression of the DNA minor groove is responsible for termination of DNA by HIV-1 reverse transcriptase. J. Mol. Biol. **285:**977–995.
30. **Le Cam, E., and E. Delain.** 1995. Nucleic acids-ligand interactions, p. 331–356. *In* G. Morel (ed.), Visualization of nucleic acids. CRC Press, Boca Raton, F1a.
31. **Le Cam, E., B. Théveny, B. Mignotte, B. Révet, and E. Delain.** 1991. Quantitative electron microscopic analysis of DNA-protein interactions. J. Electron Microsc. Tech. **18:**375–386
32. **Le Cam, E., D. Coulaud, E. Delain, P. Petitjean, B. P. Roques, D. Gerard, E. Stoylova, C. Vuilleumier, S. P. Stoylov, and Y. Mely.** 1998. Properties and growth mechanism of the ordered agregation of a model RNA by the HIV-1 nucleocapsid protein: an electron microscopy investigation. Biopolymers **45:**217–229.
33. **Lener, D., V. Tanchou, B. P. Roques, S. F. Le Grice, and J. L. Darlix.** 1998. Involvement of HIV-I nucleocapsid protein in the recruitment of reverse transcriptase into nucleoprotein complexes formed *in vitro*. J. Biol. Chem. **273:**33781–33786.
34. **Li, X., Y. Quan, E. J. Arts, Z. Li, B. D. Preston, H. de Rocquigny, B. P. Roques, J. L. Darlix, L. Kleiman, M. A. Parniak, and M. A. Wainberg.** 1996. Human immunodeficiency virus type 1 nucleocapsid protein (NCp7) directs specific initiation of minus-strand DNA synthesis primed by human tRNA(Lys3) in vitro: studies of viral RNA molecules mutated in regions that flank the primer binding site. J. Virol. **70:**4996–5004.
35. **Mansky, L. M., S. Preveral, L. Selig, R. Benarous, and S. Benichou.** 2000. The interaction of vpr with uracil DNA glycosylase modulates the human immunodeficiency virus type 1 *in vivo* mutation rate. J. Virol. **74:**7039–7047.
36. **Müller, B., T. Restle, S. Weiss, M. Gautel, G. Sczakiel, and R. S. Goody.** 1989. Co-expression of the subunits of the heterodimer of HIV-1 reverse transcriptase in *Escherichia coli*. J. Biol. Chem. **264:**13975–13978.
37. **Palaniappan, C., J. K. Kim, M. Wisniewski, P. J. Fay, and R. A. Bambara.** 1998. Control of initiation of viral plus strand DNA synthesis by HIV reverse transcriptase. J. Biol. Chem. **273:**3808–3816.
38. **Peliska, J. A., S. Balasubramanian, D. P. Giedroc, and S. J. Benkovic.** 1994. Recombinant HIV-1 nucleocapsid protein accelerates HIV-1 reverse transcriptase catalyzed DNA strand transfer reactions and modulates RNase H activity. Biochemistry **33:**13817–13823.
39. **Powell, M. D., and J. G. Levin.** 1996. Sequence and structural determinants required for priming of plus-strand DNA synthesis by the human immunodeficiency virus type 1 polypurine tract. J. Virol. **70:**5288–5296.
40. **Powell, M. D., W. A. Beard, K. Bebenek, K. J. Howard, S. F. Le Grice, T. A. Darden, T. A. Kunkel, S. H. Wilson, and J. G. Levin.** 1999. Residues in the alphaH and alphaI helices of the HIV-1 reverse transcriptase thumb subdomain required for the specificity of RNase H-catalyzed removal of the polypurine tract primer. J. Biol. Chem. **274:**19885–19893.
41. **Rein, A., L. E. Henderson, and J. G. Levin.** 1998. Nucleic-acid-chaperone activity of retroviral nucleocapsid proteins: significance for viral replication. Trends Biochem. Sci. **23:**297–301.
42. **Rumbaugh, J. A., G. M. Fuentes, and R. A. Bambara.** 1998. Processing of an HIV replication intermediate by the human DNA replication enzyme FEN1. J. Biol. Chem. **273:**28740–28745.
43. **Sambrook, J., E. F. Fritsch, and T. Maniatis.** 1989. Molecular cloning: a laboratory manual, 2nd ed. Cold Spring Harbor Laboratory Press, Cold Spring Harbor, N.Y.
44. **Stetor, S. R., J. W. Rausch, M. J. Guo, J. P. Burnham, L. R. Boone, M. J. Waring, and S. F. Le Grice.** 1999. Characterization of positive-strand initiation and termination sequences located at the center of the equine infectious anemia virus genome. Biochemistry **38:**3656–3667.
45. **Stevenson, M.** 2000. HIV nuclear import: What's the flap? Nat. Med. **6:**626–628.
46. **Telesnitsky, A., and S. P. Goff.** 1997. Reverse transcriptase and the generation of proviral DNA, p. 121–160. *In* J. M. Coffin, S. H. Hughes, and H. E. Varmus (ed.), Retroviruses. Cold Spring Harbor Laboratory Press, Cold Spring Harbor, N.Y.
47. **Tsuchihashi, Z., and P. O. Brown.** 1994. DNA strand exchange and selective DNA annealing promoted by the human immunodeficiency virus type 1 nucleocapsid protein. J. Virol. **68:**5863–5870.
48. **Unge, T., H. Ahola, R. Bhikhabhai, K. Backbro, S. Lovgren, E. M. Fenyo, A. Honigman, A. Panet, J. S. Gronowitz, and B. Strandberg.** 1990. Expression, purification, and crystallization of the HIV-1 reverse transcriptase (RT). AIDS Res. Hum. Retrovir. **6:**1297–1303.
49. **Whiting, S. H., and J. J. Champoux.** 1994. Strand displacement synthesis capability of Moloney murine leukemia virus reverse transcriptase. J. Virol. **68:**4747–4758.
50. **Whiting, S. H., and J. J. Champoux.** 1998. Properties of strand displacement synthesis by Moloney murine leukemia virus reverse transcriptase: mechanistic implications. J. Mol. Biol. **278:**559–577.
51. **Wu, T., J. Guo, J. Bess, L. E. Henderson, and J. G. Levin.** 1999. Molecular requirements for human immunodeficiency virus type 1 plus-strand transfer: analysis in reconstituted and endogenous reverse transcription systems. J. Virol. **73:**4794–4805.
52. **Wu, X., H. Liu, H. Xiao, J. A. Conway, E. Hehl, G. V. Kalpana, V. Prasad, and J. C. Kappes.** 1999. Human immunodeficiency virus type 1 integrase protein promotes reverse transcription through specific interactions with the nucleoprotein reverse transcription complex. J. Virol. **73:**2126–2135.
53. **Zennou, V., C. Petit, D. Guetard, U. Nerhbass, L. Montagnier, and P. Charneau.** 2000. HIV-1 genome nuclear import is mediated by a central DNA flap. Cell **101:**173–185.